Sensitive and convenient detection of miRNA-145 using a gold nanoparticle-HCR coupled system: computational and in vitro validations

Hanieh Beyrampour-Basmenj[1,2], Mohammad Pourhassan-Moghamddam[3,4], Sattar Akbari Nakhjavani[5], Naser Faraji[6], Mohammadreza Alivand[7], Nosratollah Zarghami[1,8], Mahnaz Talebi[9,10], Mohammad Rahmati[1,8*], Abbas Ebrahimi-Kalan[10*]

1. Department of Medical Biotechnology, School of Advanced Medical Sciences, Tabriz University of Medical Sciences, Tabriz, Iran
2. Student Research Committee, Tabriz University of Medical Sciences, Tabriz, Iran
3. School of life sciences, Faculty of Science, University of Technology Sydney, Sydney, NSW 2007, Australia.
4. ARC Research Hub for Integrated Device for End-user Analysis at Low-levels (IDEAL), Faculty of Science, University of Technology Sydney, Sydney, NSW 2007, Australia
5. Department of Molecular Medicine, School of Advanced Technologies in Medicine, Tehran University of Medical Sciences, Tehran, Iran
6. Department of Medical Nanotechnology, School of Advanced Medical Sciences, Tabriz University of Medical Sciences, Tabriz, Iran
7. Department of Genetics, Faculty of Medicine, Tabriz University of Medical Sciences, Tabriz, Iran
8. Department of Clinical Biochemistry and Laboratory Medicine, Faculty of Medicine, Tabriz University of Medical Sciences, Tabriz, Iran
9. Neurosciences Research Center (NSRC), Tabriz University of Medical Sciences, Tabriz, Iran
10. Department of Neurosciences and Cognition, School of Advanced Medical Sciences, Tabriz University of Medical Sciences, Tabriz, Iran

To whom equal correspondence should be addressed:

1- Abbas Ebrahimi-kalan: Department of Neurosciences and cognition, Faculty of Advanced Medical Sciences, Tabriz University of Medical Sciences, Tabriz, Iran.

Ebrahimiab@tbzmed.ac.ir and Abbasebra@gmail.com

2- Mohammad Rahmati: Department of Medical Biotechnology, School of Advanced Medical Sciences, Tabriz University of Medical Sciences, Tabriz, Iran

rahmatibio@gmail.com

Abstract

Multiple sclerosis (MS) remains a challenging disease that requires timely diagnosis. Therefore, an ultrasensitive optical biosensor based on hybridization chain reaction (HCR) was developed to detect microRNA-145 (miRNA-145) as an MS biomarker. To construct such a sensor, HCR occurred between specific hairpin probes, as MB1 contains a poly-cytosine nucleotide loop and MB2 has a poly-guanine nucleotide sticky end. By introducing miR-145 as a target sequence, long-range dsDNA polymers are formed. Then, positively charged gold nanoparticles (AuNPs) were incubated with the HCR product, which adsorbed onto the dsDNA polymers due to electrostatic adsorption. This resulted in the precipitation of the AuNPs. By incubating different concentrations of miR-145 with AuNPs, the changes in the UV-vis spectrum of the supernatant were analyzed. The proposed biosensor showed a great ability to detect miR-145 in a wide linear range from 1 pM–1 nM with an excellent detection limit (LOD) of 0.519 nM. Furthermore, the developed biosensor indicated considerable selectivity in discriminating between miR-145 and mismatched sequences. It shows high selectivity in differentiating targets. Interestingly, the proposed method was also able to detect miRNA-145 in the diluted serum samples. In conclusion, this sensing platform exhibits high selectivity and specificity for the detection of circulating microRNAs, which holds great promise for translation to routine clinical applications.

Keywords: Hybridization chain reaction; Colorimetric detection; miRNAs; Positively charged gold nanoparticles; Multiple sclerosis; Biosensor

1. Introduction

MicroRNAs are small non-coding RNAs that regulate gene expression and cellular processes (1). Studies show that miRNAs have great potential to be developed as diagnostic and therapeutic biomarkers for various diseases (2). Abnormal miRNAs expression in biofluids such as plasma or serum could be associated with various neurological diseases (3). Multiple sclerosis (MS) is an immune-mediated neurodegenerative disease of the central nervous system (CNS) characterized by gliosis, myelin loss, and various degrees of axonal and oligodendrocyte pathology. Due to the destructive and progressive nature of the disease, early and accurate diagnosis of MS is essential. One of the challenges in the treatment of MS is the establishment of diagnostic and treatment-associated biomarkers to identify MS patients (2). An ideal biomarker should have high sensitivity and specificity, as well as a simple, inexpensive, reproducible, and non-invasive detection method. Currently, some recognized biomarkers can help in the diagnosis and prognosis of MS, including Immunoglobulin G index, Oligoclonal bands, Chitinase-3-Like-1 precursor, Neurofilaments, and miRNAs (4).

Analysis of circulating miRNAs in the blood of MS patients showed that dysregulated levels of miR-145 could discriminate MS patients from controls with a specificity of 89.5%, a sensitivity of 90%, and an accuracy of 89.7%. Therefore, this microRNA may have diagnostic and therapeutic value in MS treatment (5, 6).

miR-145, located on chromosome 5, is a type of miRNA that's sensitive to the inflammatory response, and it's been shown deregulated in other disorders, such as inflammatory disorders, melanoma, and cancers (7, 8). It has been shown that miR-145 might also have a critical role in the development of psoriasis and can induce the inflammatory response of the skin of psoriasis patients (9).

Several detection methods have been developed to detect the expression of miRNAs, including RT-PCR, microarrays, northern blotting, electrochemical biosensors (10-13), colorimetric techniques (14-16), and isothermal amplification techniques.

Isothermal amplification techniques, including helicase-dependent amplification (HDA) (17), strand displacement amplification (SDA) (18),

loop-mediated isothermal amplification (LAMP) (19), rolling circle amplification (RCA) (20), and hybridization chain reaction (HCR) (21), can proceed at a constant temperature with technical simplicity, low cost, and high efficiency. Unlike other isothermal amplification methods, such as RCA and SDA, which require the assistance of enzymes for target detection, HCR has attracted interest because of its enzyme-free amplification strategy, single-molecule sensitivity, and entropy-driven spontaneous DNA assembly procedure (22). In HCR reactions, the monomers are designed with hairpin-like secondary structures that should coexist stably in solution until the target strands are added. The final product depends qualitatively and quantitatively on the amount of target (23-25).

To meet the requirement of ultrasensitive detection of targets, HCR is often combined with various signal transduction and colorimetric techniques (26-29). Qiu et al. (30) developed modified types of HCR hairpin probes (MB1 and MB2) containing a poly-cytosine nucleotide loop and a sticky poly-guanine nucleotide end that served as a template for the formation of fluorescent silver nanoclusters (AgNCs). They claimed that this modified reaction exhibited acceptable specificity along with AgNCs (30).

This study aims to develop a more straightforward method that does not require fluorescent readers and fluorescent materials as signal transducers. The developed method is a sensitive, simple, and rapid HCR-based reaction for the detection of miR-145 in a buffer solution and serum samples using positively charged gold nanoparticles (AuNPs) as naked-eye transducers. The signal from positive samples can also be easily quantified by measuring the optical density of the reaction solution (Fig. 1).

This article has been accepted for publication in a future issue of this journal, but has not been fully edited. Content may change prior to final publication. Citation information: DOI 10.1109/TNB.2022.3170530, IEEE Transactions on NanoBioscience

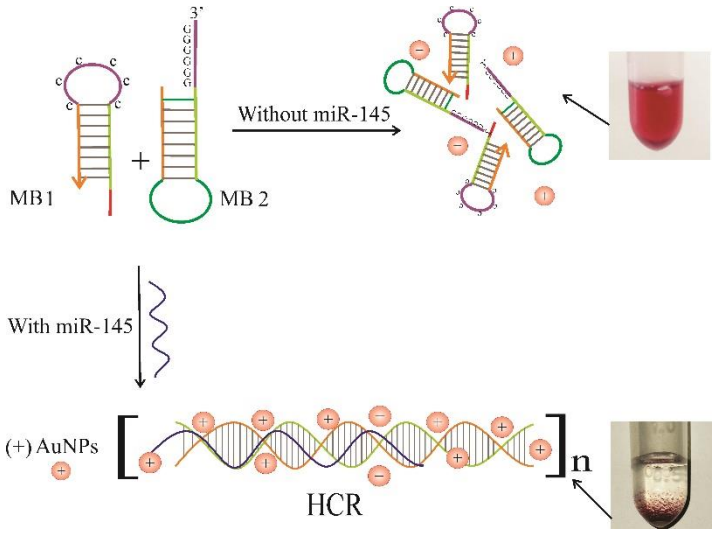

Figure 1. Graphical abstract of the proposed HCR-based sensing platform for the detection of miR-145.

2. Experimental

2.1.Chemicals

All chemicals, Hydrogen tetrachloroaurate hydrate (HAuCl4·3H2O), sodium borohydride (NaBH4), and cetyltrimethylammonium bromide (CTAB), were purchased from Merck (Germany). The sequences were designed according to the previous report (31) and synthesized by Eurofins Genomics (Germany), purified by HPLC, and dissolved in 50 mM NaAcHAc (pH 5.0) and 50.0 mM Tris-HCl (pH 7.4, containing 50 mM NaCl) as reaction buffer (Table 1). The ultrapure water used in the experiments had a resistivity of 18.2 M cm (Millipore, Billericay, USA).

Table 1. DNA sequences used in the AuNPs-based colorimetric biosensor.

Name	Sequence (5'-3')
miR-145	GTCCAGTTTTCCCAGGAATCCCT
MB1	AGGGATTCCTGGGA
	AAACTGGACCCCCCCGTCCAGTTTTCCCAGGA
MB2	GTCCAGTTTTCCCAGGAATCCCTTCC
	TGGGAAAACTGGACGGGGGG
Mismatch 1	GTCCAGTTTTCCCAGGAATGCCT
Mismatch 2	GTCCAATTTTCCCAGGAATACCT
Non-complementary	TTATTGCTTAAGAATACGCGTAG

2.2. Confirmation of MB-miRNA-145 hybrids

Gel electrophoresis was used to verify the formation of HCR amplicons in the presence of miRNA-145. A 4.0 μM MB1 and 8.0 μM MB2 stock solution was prepared and separately heated to 95 °C for 90s and cooled to 25 °C for 1 h. For the HCR reaction, 50 μL of miRNA-145 (1.0 μM) was mixed with 25 μL stock solutions of MB1 and 25 μL stock solutions of MB2 and incubated at 37 °C for 1 h with constant mixing. Three other control reactions were also prepared, including miRNA-145, MB1 alone, and an MB1/MB2 mixture without miR-145. 5 μL of each sample was mixed with 2 μL of 6x loading buffer and loaded into the lanes of a 3% agarose gel. Electrophoresis was performed at a constant potential of 85 V for 1 h in 1.0× TAE as a running buffer, followed by the gel image obtained (Quantum ST4, Fisher Biotec Pty Ltd., Australia).

2.3. Synthesis of positively charged gold nanoparticles

Based on a previous study, the best average size of AuNPs for this type of application is about 4 nm (29); therefore, in the first step, 15 mL of HAuCl4·3H2O (1.0 mM) and 2 mL of CTAB (10 mM) were mixed and stirred at room temperature for 15 min. Then 2 mL of ice-cold NaBH4 (100 mM) was added to the above solution and stirred for 15 min until the color of the solution changed from pale yellow to orange/red—the final solution was stored at 4 °C for further use.

The particle size distributions and zeta potential of the prepared AuNPs were characterized using the dynamic light scattering (DLS) technique (Zetasizer-ZS90, Malvern, UK). Transmission electron microscopy (TEM) analysis (Leo 906, Zeiss, Germany) was used to determine the size and morphology of the AuNPs at 100 kV. A Cytation5 cell imaging multi-mode reader (Bio Teck, USA) was used to detect the absorption spectrum of AuNPs in the range of 400 to 700 nm.

2.4. Measurement procedure

Different concentrations of miR-145 (1 pM-1 nM) were added to Tris-HCl buffer containing 4.0 μM MB1 and 8.0 μM MB2, and the mixture was incubated at 37 °C for 1 h with constant mixing. Then, 100 μL of the synthesized AuNPs (8.69

This article has been accepted for publication in a future issue of this journal, but has not been fully edited. Content may change prior to final publication. Citation information: DOI 10.1109/TNB.2022.3170530, IEEE Transactions on NanoBioscience

nM) were added to the above solution and incubated at 25 °C for another 2 h. Finally, 100 μL of the supernatant was collected for the UV–vis characterization.

3. Results and discussion

3.1. Biosensing principle

A critical step in HCR reactions is the selection of the correct structural features of the hairpin probes (MB1 and MB2) to ensure their kinetic properties and thermodynamic stability. The application of computational tools could be beneficial in this area. Here, we investigate the thermodynamic equilibrium, conformational entropy, and functional structures of the hairpin probes using the Vienna RNA secondary structure server (http://rna.tbi.univie.ac.at/) (32).

This server can predict the minimum free energy (MFE) of sequences. It also produces a mountain graph showing the predicted MFE and pair probabilities (position). Here, a color-coded structure with local (per base) measures is provided. Each base is colored by the positional entropy. The color of the base changes to red when the entropy of the base is at its lowest state, indicating the stability of the structures.

As Fig. 2A illustrates, both hairpin probes (MB1 and MB2) are stable in solution due to their thermodynamic stability and the low entropy of their structure (32).

The equilibrium of the system is altered by the addition of miR-145 as a target sequence, leading to a cascade of hybridization reactions and the formation of dsDNA polymers. In the absence of miR-145, the structure of the hairpin probes prevents the initiation of the reaction. miR-145 activates MB1, leading to the exposure of the short loop sequence suitable for the binding and opening of MB2. MB2 continues the cycle with another copy of MB1, and this cycle continues until all probes are consumed. In this study, the 3DNA Web server (http://web.x3dna.org/), an integrated software system for visualization and analysis of three-dimensional nucleic acid structures, was used to predict and create insights into the final product of the HCR (by inserting MB1, MB2, and miR-145 sequences) (33).

This article has been accepted for publication in a future issue of this journal, but has not been fully edited. Content may change prior to final publication. Citation information: DOI 10.1109/TNB.2022.3170530, IEEE Transactions on NanoBioscience

After modeling the three-dimensional nucleic acid structures by 3DNA, the resulting files were saved in PDB format. In addition, the 3D model of the dsDNA polymer was predicted to contain 4440 atoms.

3.1.1. Geometry Optimization

Geometry optimization is the process of determining stationary points on molecular potential energy surfaces, especially minima and transition states (34). Structural geometry was optimized using HyperChem 8.0.3 software. HyperChem is a package for performing Molecular Mechanics, Molecular Dynamics, and ab initio calculations for chemical systems. The ability to manipulate and compute properties of macromolecules such as proteins and nucleic acids is an important feature of HyperChem. Assisted Model Building with Energy Refinement (AMBER) was used as the molecular mechanic force field for Geometry Optimization.

The Polak-Ribiere was chosen as the minimization algorithm and 0.01 for the RMS (Root Mean Square) gradient is used to optimize the structure's geometry. This algorithm reduces the energy of the system by adjusting the geometric design to represent the configuration with the lowest energy. Finally, the predicted dsDNA polymer reached a steady state with an energy level of 5322.91 kcal/mol and a length of 30.9 nm. The entire structure is shown in Fig. 2B.

This article has been accepted for publication in a future issue of this journal, but has not been fully edited. Content may change prior to final publication. Citation information: DOI 10.1109/TNB.2022.3170530, IEEE Transactions on NanoBioscience

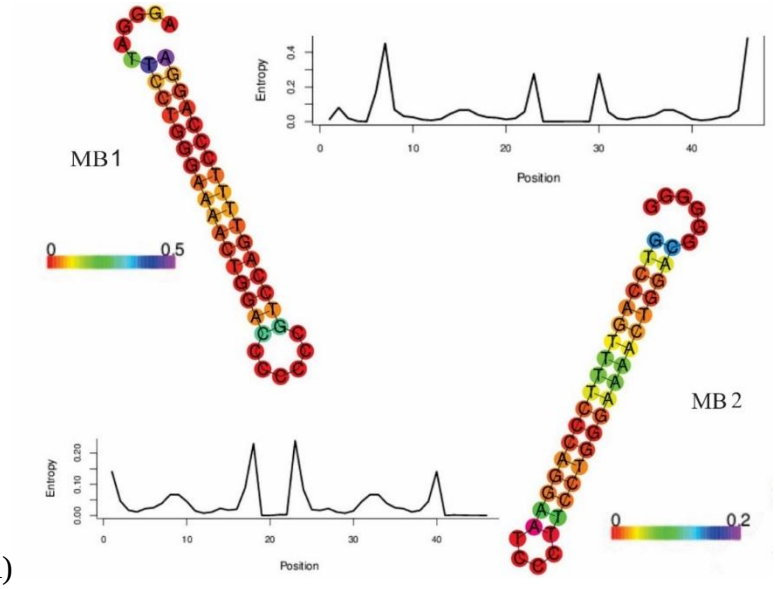

A)

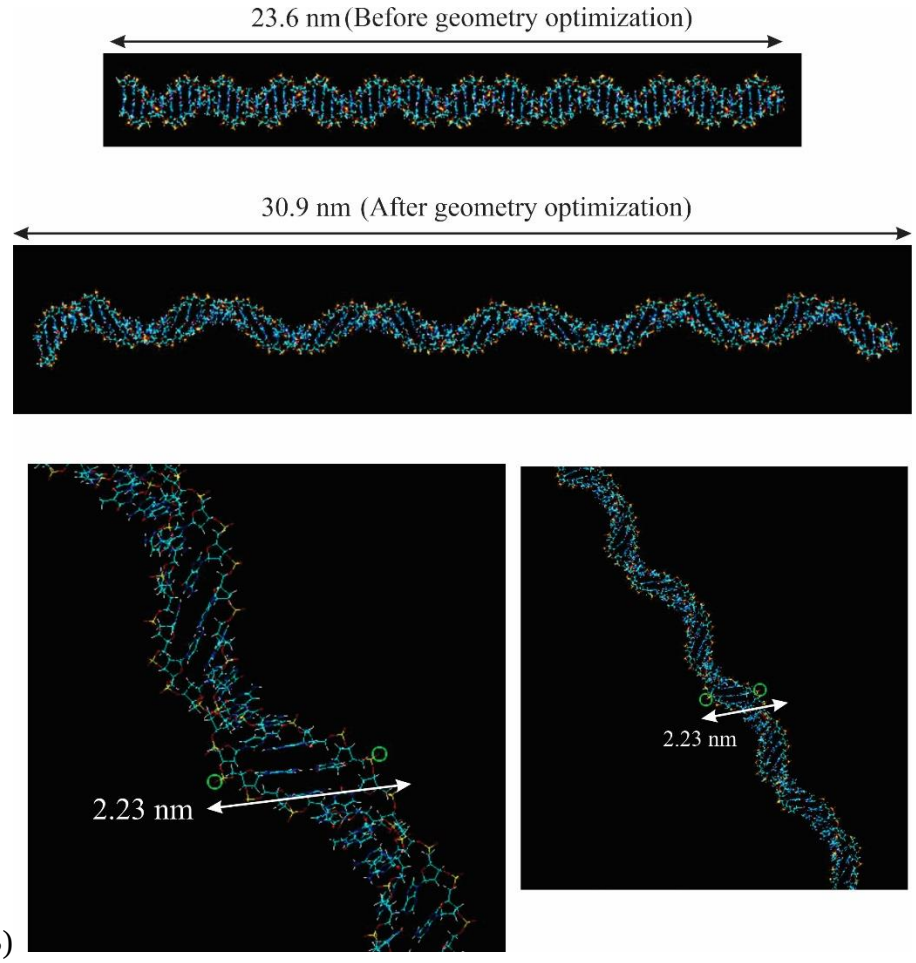

B)

Figure 2. A) Secondary structures and mountain graphs showing the entropy vs. position of the specific hairpin probes for miR-145 detection predicted by the Vienna RNA secondary structure server (32). B) Geometry Optimization of the final HCR product using HyperChem 8.0.3 software.

3.2. Characterization

Gel electrophoresis was performed to characterize the HCR reaction. As shown in Fig. 3A, incubation of miR-145 with MB1 and MB2 (lane 1) resulted in a clear smear indicating an HCR reaction. The base number of miRNA-145 was about 25 nt (lane 4), while it was about 50 nt for MB1 (lane 3), and MB1 and MB2 in the absence of miRNA-145 (lane 2), confirming that no HCR occurred between the probes in the absence of miRNA-145. The results confirmed the HCR reaction with the smear attributed to the dsDNA polymers.

Examination of the absorption spectra with different sizes of AuNPs showed that 4 nm AuNPs exhibit the best interaction between AuNPs and dsDNA polymers as HCR products (35). Therefore, a small size of AuNPs was chosen for our experiment. The average hydrodynamic diameter of the synthesized AuNPs determined by DLS was 22.58 nm, which was larger than in the TEM analysis because DLS measures the hydrodynamic radius. In contrast, the results from TEM showed a more accurate size of AuNPs (36). The zeta potential of the nanoparticles measured by DLS was positively charged.

As shown in Fig. 4A, after incubation of AuNPs with the HCR product, assimilation and precipitation of AuNPs occurred, and the average hydrodynamic diameter of AuNPs reached 157.6 nm. The zeta potential of AuNPs before incubation with the dsDNA polymers was +14.00 mV. In comparison, it decreased to +2.22 mV after incubation with the HCR products. The charge of AuNPs is decreased by their adsorption to negatively charged dsDNA polymers (Fig. 4B).

Furthermore, TEM analysis was used to investigate the properties of AuNPs before and after incubation with the HCR product. The results proved the aggregation and precipitation of AuNPs after incubation. These results directly confirm the HCR reaction between MB1 and MB2 to form dsDNA, which leads to the precipitation of AuNPs (Fig. 3B).

This article has been accepted for publication in a future issue of this journal, but has not been fully edited. Content may change prior to final publication. Citation information: DOI 10.1109/TNB.2022.3170530, IEEE Transactions on NanoBioscience

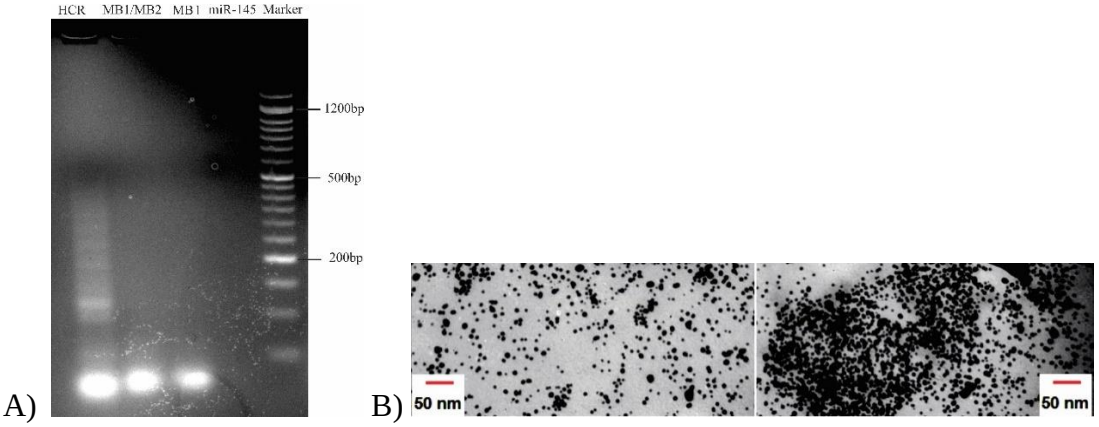

Figure 3. A) The gel electrophoresis images of the HCR-based assay, lane 1 from left: HCR product with 1.0μM miR-145 reacted with MB1/MB2 mixture (1:2 ratio), lane 2: MB1/MB2 mixture in the absence of miR-145, lane 3: 1.0μM MB1, lane 4: miR-145, and lane 5: DNA marker. B) TEM images of AuNPs-based colorimetric biosensor before (left) and after (right) incubation with HCR product.

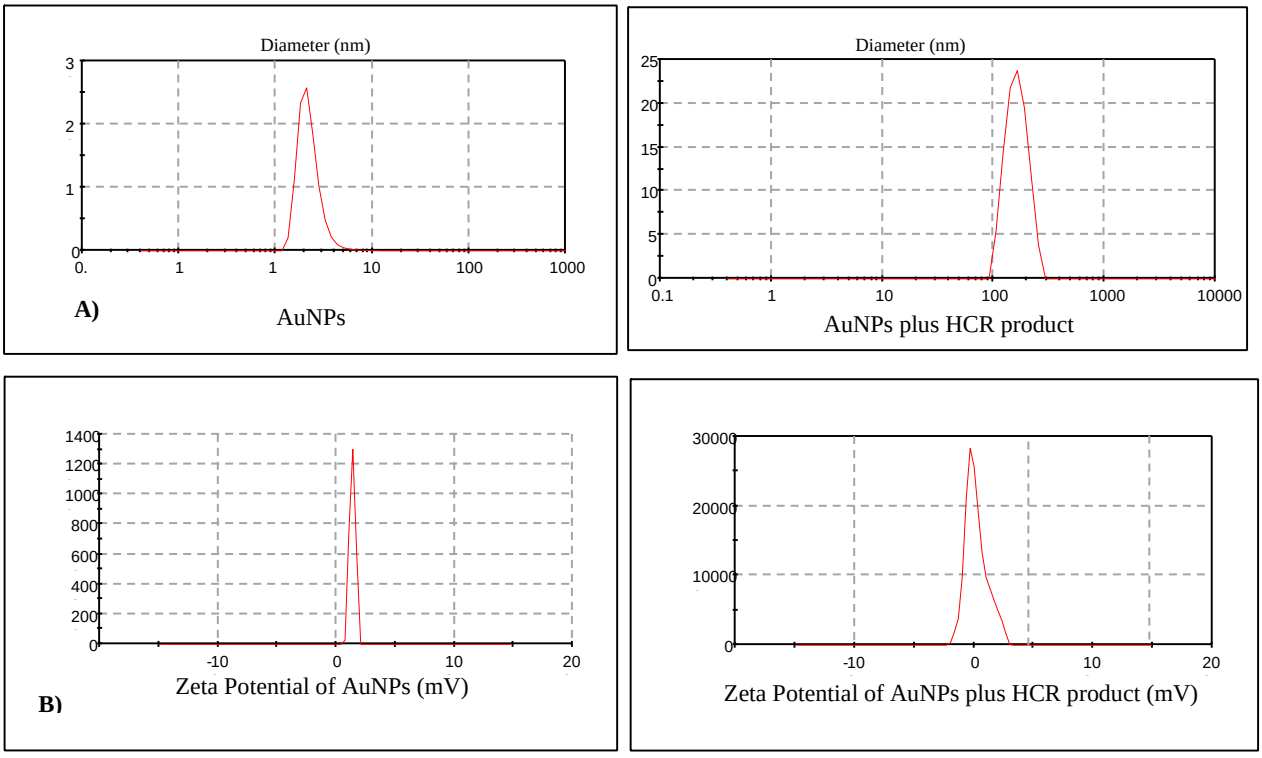

Figure 4. (A) DLS results of AuNPs before and after incubation with MB1/MB2 mixture (1:2 ratio) and 10nM target miR-145. (B) Zeta potential analysis of AuNPs before and after incubation with HCR product.

3.3. Analytical performance

The UV-vis absorption spectra of AuNPs in the supernatant showed that as the concentration of miR-145 increased, the length of dsDNA polymers as HCR product increased and the amount of precipitated AuNPs increased due to electrostatic adsorption, resulting in a decrease in the absorption spectra of the supernatant. This gold nanoparticle-HCR coupled system is specifically designed for miRNA-145, which is one of the most up-regulated miRNAs in MS patients. Different miRNAs are deregulated in MS but cannot initiate the reaction due to the HCR's specificity. Just the adsorption spectra of AuNPs can show slight but not significant changes due to electrostatic adsorption.

The UV–vis absorption spectra of miR-145 at different concentrations from 1 pM to 1 nM are shown in Fig. 5A. The absorption spectra at 525 nm decreased with increasing amount of the target**.** Data analysis showed a linear detection range for miR-145 concentrations from 1 pM to 1 nM with the linear regression equation $y = -0.021\ln(x) + 0.1922$ ($R2=0.9877$). The detection limit was calculated to be 0.519 nM using the formulas: $LoD = LoB + 1.645(SD_{\text{low concentration sample}})$ and $LoB = \text{mean}_{\text{blank}} + 1.645(SD_{\text{blank}})$ (Fig. 5B) (37). Moreover, our sensing strategy was simple and did not require the use of an enzyme or a costly device, making our biosensor more suitable than existing enzyme-based methods (Table 3).

This article has been accepted for publication in a future issue of this journal, but has not been fully edited. Content may change prior to final publication. Citation information: DOI 10.1109/TNB.2022.3170530, IEEE Transactions on NanoBioscience

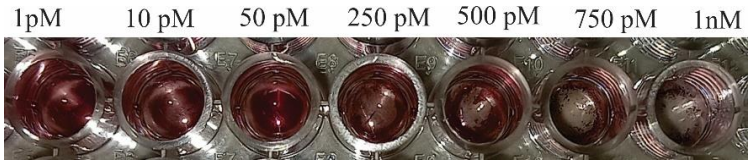

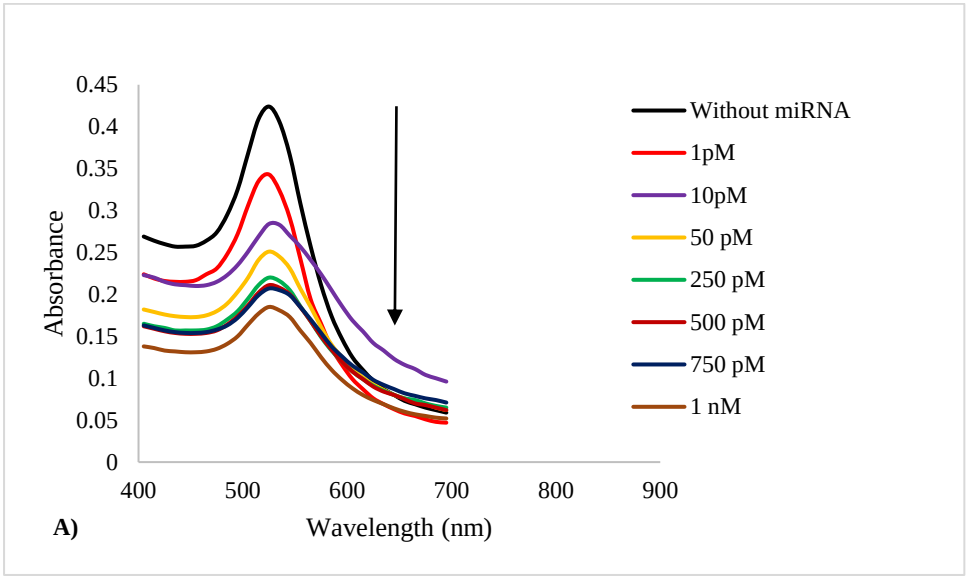

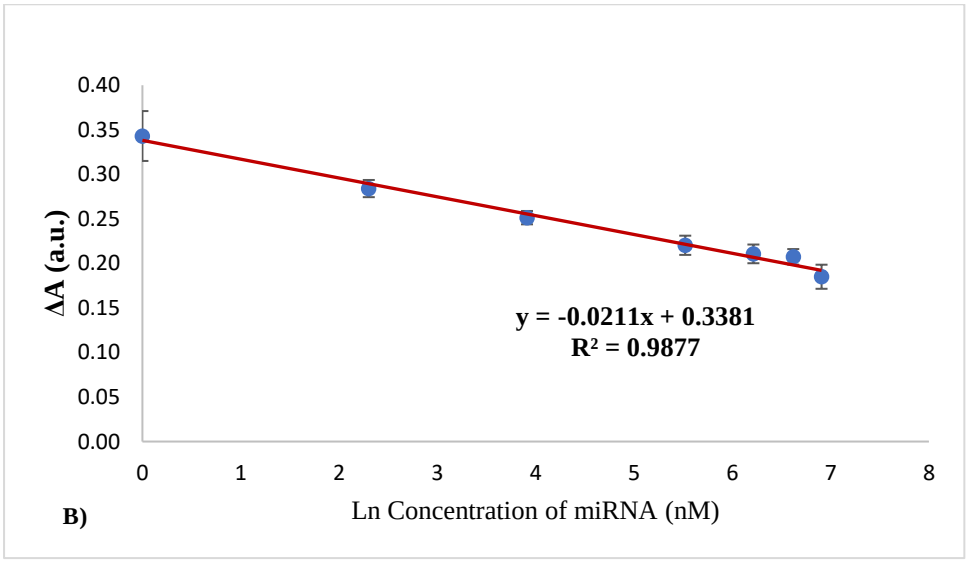

Figure 5. A) UV–vis absorption of the AuNPs-based colorimetric detection in the presence of different concentrations of miR-145. B) The calibration curve of different Ln concentrations of miR-145.

3.4. Real Sample Analysis

Due to the importance of early and accurate diagnosis of MS and to evaluate the feasibility of the proposed method for the detection of miRNA-145 in biological samples, human serum samples were collected according to the ethics guidelines approved by the ethics committee of Tabriz University of medical sciences and diluted 50 times with reaction buffer. To prepare serum sample, the blood was taken from a healthy woman (age 27) collected in a tube without any additives. The sample centrifuged at 4 °C at 3000 rpm for 10 min and the serum was isolated.

Then, 50 pM, 500 pM, and 750 pM miR-145 were mixed with 25 µl MB1 and MB2 mixture (1:2 ratio) and incubated with the diluted serum samples at 37 °C for 1 h with constant mixing. Similar to the experiment, 100 µL AuNPs were added to the samples and incubated for another 2 h. Finally, UV-vis spectrum analysis was used to characterize the concentrations of AuNPs in the supernatant, and the detected miR-145 concentrations were calculated from the calibration curve using the linear regression equation. The recovery experiments were performed. As shown in Table 2, excellent recovery was obtained. The results confirmed the potential of the proposed colorimetric sensing platform for the detection of miR-145 in biological samples.

According to studies, miR-145 is increased in MS patients' blood samples three-fold compared to non-MS subjects (38, 39). This indicates that our suggested biosensor should produce higher signals (three times) from the patient samples. So, it is expected that healthy samples result in low signals.

Table 2. miRNA-145 detection in serum samples (n=3).

Sample	Added	Found	Recovery (%)	RSD (%)
1	50 pM	2.51	83.92	6.24
2	500 pM	0.657	94.82	2.447
3	750 pM	0.28	95.89	3.797

3.5. Selectivity of the sensor

To evaluate the specificity and selectivity of the AuNPs-based HCR method, three types of sequences were prepared: one-base mismatched, two-base mismatched, and a non-complementary (10 nM) (Table 1). To determine the selectivity of the sensor in detecting miR-145, UV-vis absorption spectra changes (ΔA) of AuNPs after HCR reaction with miR-145, mismatch 1, mismatch 2, and non-complementary targets were examined. As shown in Fig. 6, these mismatched sequences fail to generate HCR reaction, which is confirmed by the absorbance variations between samples. The reduction in absorption spectra was statistically more significant than for the mismatched and random sequence (P-Value <0.05). The results showed that the proposed HCR-based platform has high selectivity and specificity for the detection of miRNAs with AuNPs.

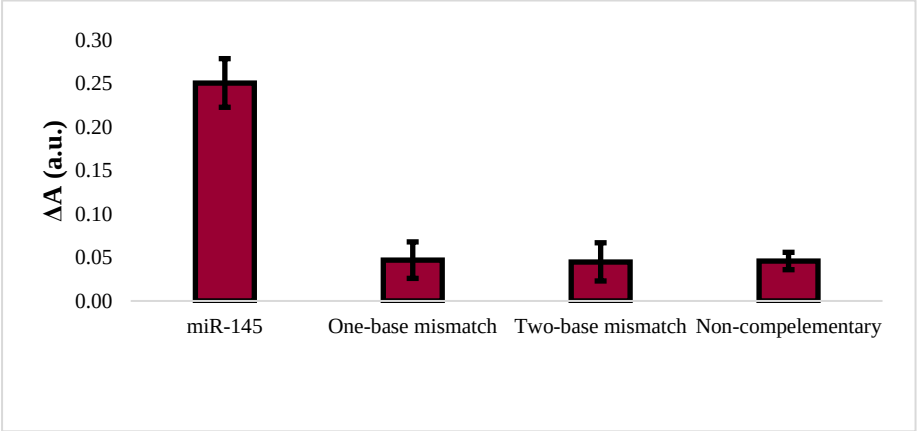

Figure 6. Selectivity and specificity of the colorimetric biosensor against mismatched target sequences (1) miR-145 as target sequence; (2) one-base mismatch; (3) two-base mismatch; (4) non-complementary.

Table 3. Comparison of our method with other related miRNA detection methods.

Material	Linear range	LOD	REF.
Graphene/AuNPs	10 nM-0.98 μM	3.2 nM	(40)
AuNPs	20 pM-10 nM	6.8 pM	(29)
Gold nanorods	0-60 nM	1.47 nM	(14)
Silver nanoclusters	5.0 nM-125 nM	1.7 nM	(41)
Silver nanoclusters	1.56-400 nM	0.78 nM	(30)
(+)AuNPs	1 pM-1 nM	0.519 nM	Our work

4. Conclusion

miR-145 as a MS biomarker could support diagnostics of the disease. A cascade of hybridization reactions with oligonucleotide-designed hairpin probes (30) was employed to readily detect changes in miR-145 levels using AuNPs aggregation as a signal transduction strategy. The developed colorimetric biosensor showed a wide linear range from 1 pM to 1 nM and a low detection limit of 0.519 nM under optimal conditions. The selectivity of the developed biosensor enabled the discrimination of miRNA-145 at single-base level. Analysis in real serum samples showed good recovery results, indicating the potential of our sensing platform for detecting in complex biological fluids and using it for detection of various nucleic acid-based biomarkers.

Acknowledgment

We would like to thank the Tabriz University of Medical Sciences, Tabriz, Iran, for providing financial (Grant NO. IR.TBZMED.REC.1398.566) and instrumental supports.

References

1. Li Z, Rana TM. Therapeutic targeting of microRNAs: current status and future challenges. Nature reviews Drug discovery. 2014;13(8):622-38.
2. Teunissen CE, Malekzadeh A, Leurs C, Bridel C, Killestein J. Body fluid biomarkers for multiple sclerosis—the long road to clinical application. Nature Reviews Neurology. 2015;11(10):585.
3. Junker A, Hohlfeld R, Meinl E. The emerging role of microRNAs in multiple sclerosis. Nature Reviews Neurology. 2011;7(1):56-9.
4. Mathur D, Mishra BK, Rout S, Lopez-Iranzo FJ, Lopez-Rodas G, Vallamkondu J, et al. Potential Biomarkers Associated with Multiple Sclerosis Pathology. International journal of molecular sciences. 2021;22(19).
5. Keller A, Leidinger P, Lange J, Borries A, Schroers H, Scheffler M, et al. Multiple sclerosis: microRNA expression profiles accurately differentiate patients with relapsing-remitting disease from healthy controls. PloS one. 2009;4(10):e7440.
6. Guerau-de-Arellano M, Alder H, Ozer HG, Lovett-Racke A, Racke MK. miRNA profiling for biomarker discovery in multiple sclerosis: from microarray to deep sequencing. Journal of neuroimmunology. 2012;248(1-2):32-9.
7. Liu S, Gao G, Yan D, Chen X, Yao X, Guo S, et al. Effects of miR-145-5p through NRAS on the cell proliferation, apoptosis, migration, and invasion in melanoma by inhibiting MAPK and PI3K/AKT pathways. Cancer medicine. 2017;6(4):819-33.
8. Balachandran AA, Larcher LM, Chen S, Veedu RN. Therapeutically Significant MicroRNAs in Primary and Metastatic Brain Malignancies. Cancers. 2020;12(9).
9. Wang Y, Cao Y. miR-145-5p inhibits psoriasis progression by regulating the Wnt/β-catenin pathway. American journal of translational research. 2021;13(9):10439-48.
10. Li F, Peng J, Zheng Q, Guo X, Tang H, Yao S. Carbon nanotube-polyamidoamine dendrimer hybrid-modified electrodes for highly sensitive electrochemical detection of microRNA24. Analytical chemistry. 2015;87(9):4806-13.
11. Zhang Y, Yan Y, Chen W, Cheng W, Li S, Ding X, et al. A simple electrochemical biosensor for highly sensitive and specific detection of microRNA based on mismatched catalytic hairpin assembly. Biosensors and Bioelectronics. 2015;68:343-9.
12. Peltier HJ, Latham GJ. Normalization of microRNA expression levels in quantitative RT-PCR assays: identification of suitable reference RNA targets in normal and cancerous human solid tissues. RNA (New York, NY). 2008;14(5):844-52.
13. Chan JA, Krichevsky AM, Kosik KS. MicroRNA-21 is an antiapoptotic factor in human glioblastoma cells. Cancer Res. 2005;65(14):6029-33.
14. Xu C, Lan L, Yao Y, Ping J, Li Y, Ying Y. An unmodified gold nanorods-based DNA colorimetric biosensor with enzyme-free hybridization chain reaction amplification. Sensors and Actuators B: Chemical. 2018;273:642-8.
15. Chen C, Tan R, Wong L, Fekete R, Halsey J. Quantitation of microRNAs by real-time RT-qPCR. PCR protocols: Springer; 2011. p. 113-34.
16. Smith SM, Murray DW. An overview of microRNA methods: expression profiling and target identification. Molecular Profiling. 2012:119-38

17. Vincent M, Xu Y, Kong H. Helicase-dependent isothermal DNA amplification. EMBO reports. 2004;5(8):795-800.
18. Wang C, Zhou H, Zhu W, Li H, Jiang J, Shen G, et al. Ultrasensitive electrochemical DNA detection based on dual amplification of circular strand-displacement polymerase reaction and hybridization chain reaction. Biosensors and Bioelectronics. 2013;47:324-8.
19. Notomi T, Okayama H, Masubuchi H, Yonekawa T, Watanabe K, Amino N, et al. Loop-mediated isothermal amplification of DNA. Nucleic acids research. 2000;28(12):e63-e.
20. Zhao W, Ali MM, Brook MA, Li Y. Rolling circle amplification: applications in nanotechnology and biodetection with functional nucleic acids. Angewandte Chemie International Edition. 2008;47(34):6330-7.
21. Torrente-Rodríguez R, Campuzano S, Montiel VR-V, Montoya J, Pingarrón J. Sensitive electrochemical determination of miRNAs based on a sandwich assay onto magnetic microcarriers and hybridization chain reaction amplification. Biosensors and Bioelectronics. 2016;86:516-21.
22. Dirks RM, Pierce NA. Triggered amplification by hybridization chain reaction. Proceedings of the National Academy of Sciences. 2004;101(43):15275-8.
23. Miti A, Zuccheri G. Hybridization chain reaction design and biosensor implementation. DNA Nanotechnology: Springer; 2018. p. 115-35.
24. Kanat B, Portakal HS, Doluca O, editors. Demonstration of G-quadruplex-assisted hybridization chain reaction for nucleic acid detection. 2020 Medical Technologies Congress (TIPTEKNO); 2020: IEEE.
25. Nishimura T, Yamada K, Ohno Y, Ogura Y, Tanida J, editors. Amplification and encoding of biomolecular signals with designed reactions of DNA. The 6th 2013 Biomedical Engineering International Conference; 2013: IEEE.
26. Li S, Li H, Li X, Zhu M, Li H, Xia F. Hybridization Chain Reaction-Amplified Electrochemical DNA-Based Sensors Enable Calibration-Free Measurements of Nucleic Acids Directly in Whole Blood. Anal Chem. 2021;93(23):8354-61.
27. Chen W, Zhang X, Li J, Chen L, Wang N, Yu S, et al. Colorimetric Detection of Nucleic Acids through Triplex-Hybridization Chain Reaction and DNA-Controlled Growth of Platinum Nanoparticles on Graphene Oxide. Anal Chem. 2020;92(3):2714-21.
28. Huang Z, He D, Li HW. A fluorometric assay of thrombin using magnetic nanoparticles and enzyme-free hybridization chain reaction. Mikrochimica acta. 2020;187(5):295.
29. Miao X, Ning X, Li Z, Cheng Z. Sensitive detection of miRNA by using hybridization chain reaction coupled with positively charged gold nanoparticles. Sci Rep. 2016;6:32358.
30. Qiu X, Wang P, Cao Z. Hybridization chain reaction modulated DNA-hosted silver nanoclusters for fluorescent identification of single nucleotide polymorphisms in the let-7 miRNA family. Biosensors and Bioelectronics. 2014;60:351-7.
31. Mansourian N, Rahaie M, Hosseini M. A Nanobiosensor based on fluorescent DNA-hosted silver nanocluster and HCR amplification for detection of MicroRNA involved in progression of multiple sclerosis. Journal of fluorescence. 2017;27(5):1679-85.
32. Hofacker IL. Vienna RNA secondary structure server. Nucleic acids research. 2003;31(13):3429-31.
33. Lu X-J, Olson WK. 3DNA: a versatile, integrated software system for the analysis, rebuilding and visualization of three-dimensional nucleic-acid structures. Nature protocols. 2008;3(7):1213.
34. Q-CHEM. A geometry optimization with q-chem 2021,JUNE 13 [Available from: https://manual.q-chem.com/5.4/A1.S1.html.
35. Miao X, Ning X, Li Z, Cheng Z. Sensitive detection of miRNA by using hybridization chain reaction coupled with positively charged gold nanoparticles. Scientific reports. 2016;6(1):1-9.

36. Sikkema FD, Comellas-Aragonès M, Fokkink RG, Verduin BJ, Cornelissen JJ, Nolte RJ. Monodisperse polymer-virus hybrid nanoparticles. Organic & biomolecular chemistry. 2007;5(1):54-7.
37. Armbruster DA, Pry T. Limit of blank, limit of detection and limit of quantitation. The Clinical biochemist Reviews. 2008;29 Suppl 1(Suppl 1):S49-52.
38. Søndergaard HB, Hesse D, Krakauer M, Sørensen PS, Sellebjerg F. Differential microRNA expression in blood in multiple sclerosis. Multiple sclerosis (Houndmills, Basingstoke, England). 2013;19(14):1849-57.
39. Sharaf-Eldin WE, Kishk NA, Gad YZ, Hassan H, Ali MAM, Zaki MS, et al. Extracellular miR-145, miR-223 and miR-326 expression signature allow for differential diagnosis of immune-mediated neuroinflammatory diseases. Journal of the neurological sciences. 2017;383:188-98.
40. Zhao H, Qu Y, Yuan F, Quan X. A visible and label-free colorimetric sensor for miRNA-21 detection based on peroxidase-like activity of graphene/gold-nanoparticle hybrids. Analytical Methods. 2016;8(9):2005-12.
41. Xia X, Hao Y, Hu S, Wang J. Hairpin DNA probe with 5'-TCC/CCC-3' overhangs for the creation of silver nanoclusters and miRNA assay. Biosensors and Bioelectronics. 2014;51:36-9.